

Information Circular 9272

**Summary of Combustion Products
From Mine Materials: Their
Relevance to Mine Fire Detection**

By Margaret R. Egan

**UNITED STATES DEPARTMENT OF THE INTERIOR
Manuel Lujan, Jr., Secretary**

**BUREAU OF MINES
T S Ary, Director**

Library of Congress Cataloging in Publication Data:

Egan, Margaret R.

Summary of combustion products from mine materials : their relevance to mine fire detection / by Margaret R. Egan.

p. cm. — (Bureau of Mines information circular; 9272)

Includes bibliographical references (p. 11).

Supt. of Docs. no.: I 28.27:9272.

1. Mine fires. 2. Combustion gases. I. Title. II. Series: Information circular (United States. Bureau of Mines); 9272.

TN295.U4 [TN315] 622 s—dc20 [622'.8] 90-2488 CIP

CONTENTS

	<i>Page</i>
Abstract	1
Introduction	2
Experimental methods and materials	2
Intermediate-scale fire tunnel	4
Calculations	5
Production parameters	5
Heat-release rates	5
Smoke intensity parameters	6
Smoke particle diameters	7
Combustion hazards	7
Fire detection	9
Conclusions	11
References	11
Appendix.—Symbols used in this report	12

ILLUSTRATIONS

1. Wood crib configurations	3
2. Schematic of intermediate-scale fire tunnel and data-acquisition system	4

TABLES

1. Materials, ignition sources, ventilation rates, mass-loss rates, major elemental constituents, ash, and heating values.	2
2. Heat-release equation variables	6
3. Gas concentrations, gas ratios, heat-release rates, and heats of combustion	7
4. Smoke characteristics	8
5. Relative gas and smoke values from flaming combustion	9
6. Production constants from flaming combustion	9
7. Production yields from flaming combustion	9
8. Sensor alarm ratios and fire intensity at sensor alarm for flaming combustion	10
9. Relative levels of CO and smoke at respective alarm thresholds for smoldering combustion	11
10. Detectability ranking of smoldering mine combustibles	11

UNIT OF MEASURE ABBREVIATIONS USED IN THIS REPORT

Btu/lb	British thermal unit per pound	m	meter
°C	degree Celsius	m ⁻¹	reciprocal meter
cm	centimeter	m ² /g	square meter per gram
cm ³	cubic centimeter	mg/m ³	milligram per cubic meter
g	gram	min	minute
g/cm ³	gram per cubic centimeter	mm	millimeter
g/g	gram per gram	μm	micrometer
g/kJ	gram per kilojoule	m ³ /s	cubic meter per second
g/(m ³ ·ppm)	gram per cubic meter times part per million	p/cm ³	particle per cubic centimeter
g/s	gram per second	pct	percent
kg	kilogram	p/g	particle per gram
kJ/g	kilojoule per gram	p/kJ	particle per kilojoule
kJ/m ³	kilojoule per cubic meter	p/s	particle per second
kW	kilowatt	ppm	part per million

SUMMARY OF COMBUSTION PRODUCTS FROM MINE MATERIALS: THEIR RELEVANCE TO MINE FIRE DETECTION

By Margaret R. Egan¹

ABSTRACT

The U.S. Bureau of Mines investigated the product-of-combustion (POC) characteristics of combustible materials used in typical coal mining operations in a series of experiments conducted in an intermediate-scale fire tunnel. The materials examined include wood cribs, transformer fluid, coal, conveyor belting, brattice cloth, and ventilation ducting.

Smoke and toxic gases evolved from burning materials contribute to panic conditions and hinder escape. Smoke irritates and obscures vision, while toxic gases physically debilitate and disorient the victims. However, POC emissions may be used for early warning fire detection. POC levels will vary not only between materials but also between stages of combustion and the conditions in which they are burning. This report summarizes the POC characteristics of each material and evaluates their effectiveness for early warning mine fire detection. Results show that smoke was the POC most readily detected from the smoldering materials tested.

¹Research chemist, Pittsburgh Research Center, U.S. Bureau of Mines, Pittsburgh, PA.

INTRODUCTION

These studies were undertaken by the U.S. Bureau of Mines to determine the levels and detectability of the POC from various mine combustibles. Ventilated mine conditions were simulated in an intermediate-scale fire tunnel. This report includes and expands upon data from previous studies (1-5)² in which the POC of these materials were examined separately.

The goals of this research are to develop more reliable and sensitive mine fire sensors using the most efficient and effective methods available and to determine the levels of smoke and toxic gases produced from different types of combustibles in fires. To achieve these goals, the POC levels of the potential fuels must be evaluated experimentally.

Toxic gas can incapacitate victims far removed from the actual fire. Smoke, when liberated in any quantity, presents serious problems of obscuration delaying evacuation and rescue. However, smoke and gas provide

²Italic numbers in parentheses refer to items in the list of references preceding the appendix at the end of this report.

measurable products that can be detected when the fire is smoldering or flaming. The POC levels are related to fundamental differences in the materials, such as physical state (solid or liquid), origin (natural or synthetic), chemical composition (which may vary according to source or manufacturer), and the fire conditions (oxygen supply).

The objectives of this report are (1) to explore the hazardous POC generated from selected mine materials, (2) to examine the relative detectabilities of these products, (3) to provide data on the performance of materials in a fire, and (4) to provide data which could be used to develop reliable and sensitive early warning fire detectors. The measurements include: ventilation rate (V_oA_o), mass-loss rate ($\Delta m/\Delta t$), gas concentrations, smoke particulate mass (M_o) and number (N_o) concentrations, and light transmission (T) through smoke. From these results, the following parameters can be calculated: heat-release rate (\dot{Q}_A), generation rates (\dot{G}_X), production yields (Y_X), production constants (β_X), particle diameters (d_m) and (d_{32}), and optical density (OD).

EXPERIMENTAL METHODS AND MATERIALS

Two important factors influencing mine fire environments are heat and air velocity. The selection of the ignition source depended upon the fire response characteristics of the material. Smoldering materials (those from which flames did not erupt or propagate) were pyrolyzed using three electric strip heaters. Materials that readily spread flame were ignited with a natural gas flame. Table 1 lists the ignition sources, V_oA_o , $\Delta m/\Delta t$, major elemental constituents, ash, and heating values for the mine combustibles tested.

The following materials were examined in this study:

- (1) Wood cribs: Four configurations of wood cribs were tested in duplicate. The height and spacing of the sticks were chosen to study the growth and the propagation of the fire. The cribs weighed approximately 2 kg and were constructed of Douglas fir using a small amount of carpenter's glue for joining. The configurations and their dimensions are shown in figure 1.

Table 1.—Materials, ignition sources, ventilation rates, mass-loss rates, major elemental constituents, ash, and heating values

Material	Ignition source	V_oA_o , m ³ /s	$\Delta m/\Delta t$, g/s	C, pct	H, pct	Ash, pct	Cl, pct	Heating value, Btu/lb
Wood	Gas jet	1.0	10.38	46.4	6.5	ND	ND	7,564
Transformer fluid	do.	.47	.87	ND	ND	ND	ND	18,200
Coal	Strip heaters	.24	.39	78.0	5.3	5.6	ND	13,947
SBR belts	Gas jet	.11	2.37	68.0	6.4	12.2	3.9	13,327
NP belts	do.	.11	.89	52.9	4.9	14.9	13.0	10,004
PVC belts	do.	.11	.21	51.8	6.2	5.6	18.3	10,524
PVC brattice	Strip heaters	.16	¹ .09	47.5	5.5	7.1	30.4	10,096
Jute brattice	do.	.16	¹ .25	33.9	6.0	9.6	7.3	5,845
Ventilation ducting	do.	.15	.44	22.4	2.0	59.8	² <1.5	3,856

ND not determined.

¹Results from thermal degradation, not flaming combustion.

²Bromine content = 7.0 pct.

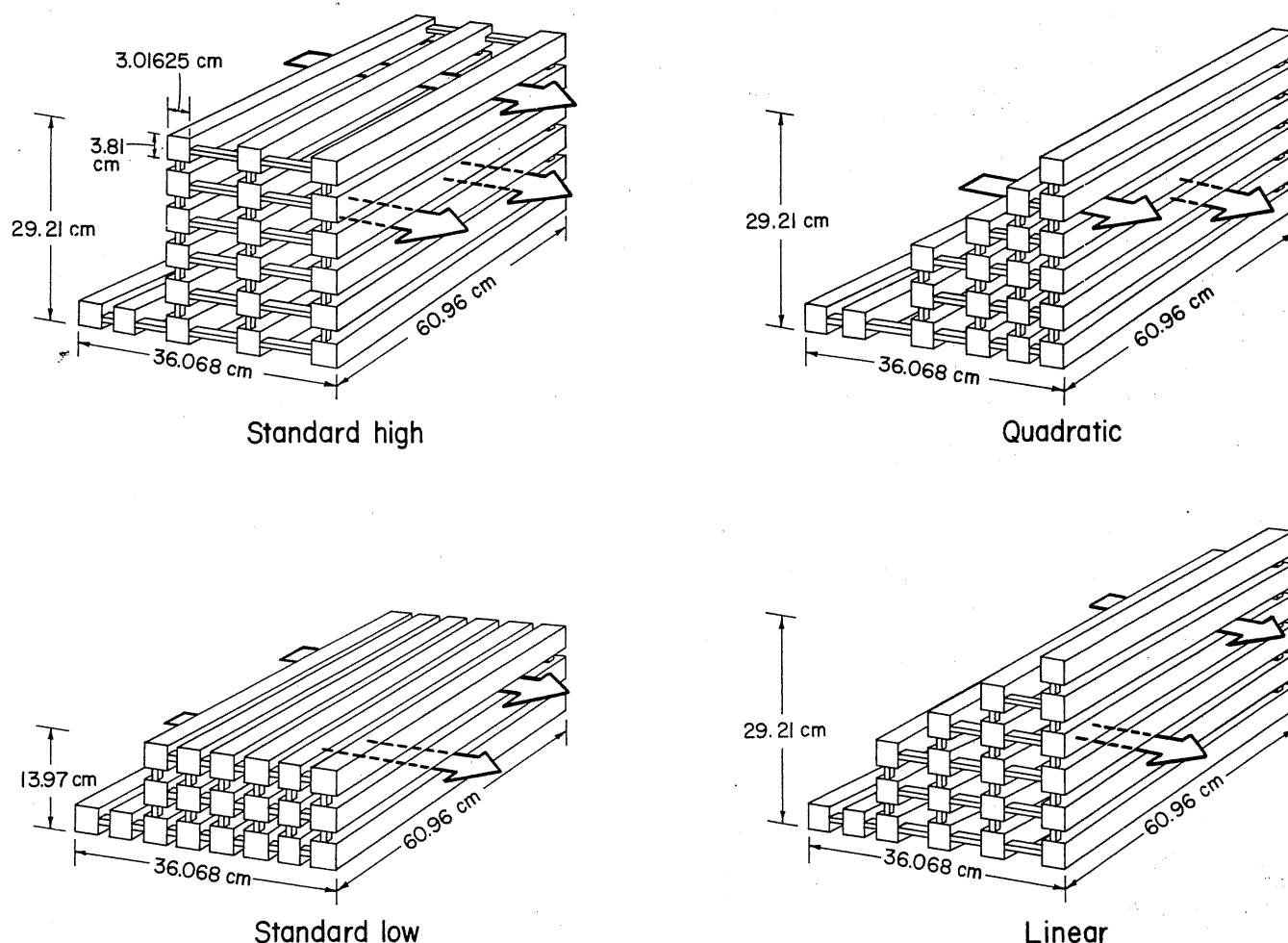


Figure 1.—Wood crib configurations. Air flows in direction of arrows.

(2) Transformer fluid: Ten experiments were completed using three commercially available brands of transformer fluid—four with brand A and three with brands B and C. A 25-cm-diam pan filled with transformer fluid to a depth of 2.5 cm was used for each experiment. The natural gas jet flame was turned off once the transformer fluid had ignited. The flames spread quickly, engulfing the entire fuel surface within 1 min and remained visible for approximately 30 min.

(3) Coal: Bituminous coal from the Pittsburgh Seam was used for all six experiments. Approximately 18 kg of coal was broken into pieces measuring 125 cm³ or less and placed in a 59- by 68-cm stainless steel pan. Three strip heaters were equidistantly imbedded approximately 2.5 cm beneath the surface of the coal. In this configuration, the coal smoldered for 9 min before flames erupted. The smoldering data were compiled during this preflaming period.

(4) Conveyor belts: A 23- by 30-cm section of each belt was tested in duplicate. The belts were classified according to covering. They included four different styrene butadiene rubber (SBR) belts, two neoprene (NP) belts, and four polyvinyl chloride (PVC) belts. Once the gas burner was extinguished, the SBR belts sustained flaming combustion from 26 to 52 min, the NP belts from 15 to 18 min, and the PVC belts from 3 to 15 min. The high chlorine content of the PVC belts accounts for their self-extinguishing tendency. However, none of the belts were totally consumed.

(5) Brattice cloth: Fourteen different PVC brattice cloths from several manufacturers and one sample of treated jute were tested in duplicate. A double thickness of brattice measuring 20- by 40-cm was placed on a wire mesh, which rested on three strip heaters. The thermal decomposition of PVC brattice cloth did not result in flaming combustion. The results listed under smoldering

combustion were actually the peak emission levels. This occurred from the 15th through the 19th min after the strip heaters were turned on. After this period, the emission levels gradually decreased. The jute experiments were conducted under the same conditions as the PVC brattice experiments. Although jute is a woody fiber and can burn, the temperature was not high enough to ignite it. The jute smoldered and reached its peak emissions from the 15th through the 20th min.

(6) Ventilation ducting: Eight types of rigid fiberglass reinforced polyester resin ducting from several manufacturers were tested in triplicate. The reinforcing

glass fibers contributed to the physical integrity by assuring certain minimum levels of solid residue. The polyester components of these ducts are combustible and even with fire-prevention additives, they can still erupt into flames given the proper conditions. The samples ranged in thickness from 2 to 5 mm. All but one was cylindrical with a diameter of either 41 or 46 cm. A sample 20- by 40-cm rested on three strip heaters. The ducting smoldered for 5 min. Flaming combustion lasted about 10 min. The polyester resin coating charred or completely burned leaving only strands of fiberglass.

INTERMEDIATE-SCALE FIRE TUNNEL

The Bureau's ventilated intermediate-scale fire tunnel was used to simulate a ventilated mine entry. Figure 2 shows a schematic view of the tunnel with its data acquisition system. The tunnel specifications, test

equipment, and procedures are presented in full detail in previous reports (1-5). Smoke and effluent gases were continuously sampled at the same location in the tunnel. The instrument readings were recorded every minute.

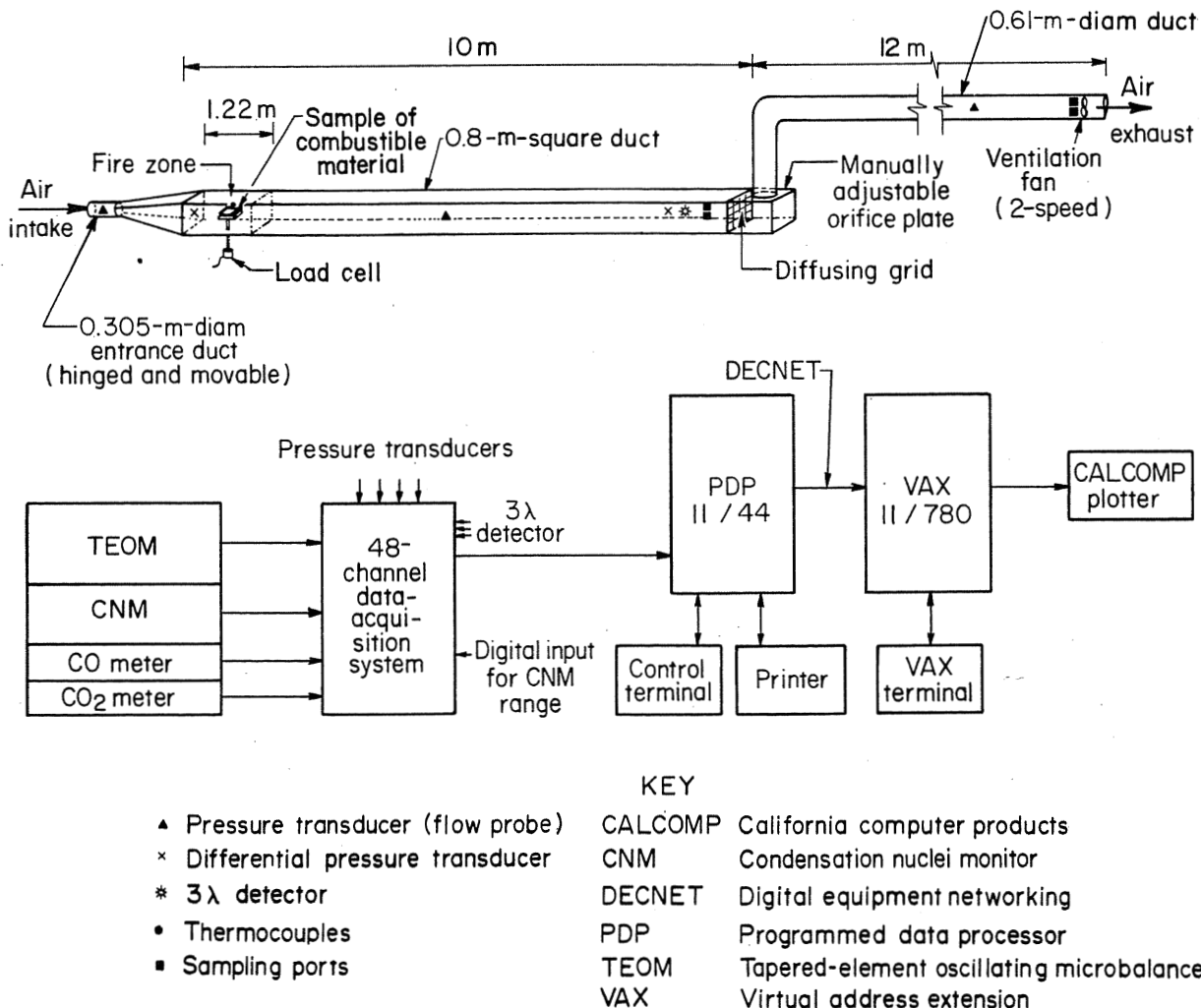


Figure 2.—Schematic of Intermediate-scale fire tunnel (top) and data-acquisition system (bottom).

CALCULATIONS

For the evaluation of detectability, the following determinations were considered to be important: \dot{G}_x , Y_x , β_x , relative values, \dot{Q}_A , d_m and d_{32} , and smoke obscuration and OD.

PRODUCTION PARAMETERS

The \dot{G}_x of a product is related to its measured concentration and V_oA_o by the general expression

$$\dot{G}_x = M_x (V_oA_o) (\Delta X) \quad (1)$$

where $M_{CO_2} = 1.97 \times 10^{-3} \text{ g}/(\text{m}^3 \cdot \text{ppm})$,

$$M_{CO} = 1.25 \times 10^{-3} \text{ g}/(\text{m}^3 \cdot \text{ppm}),$$

$$V_oA_o = \text{ventilation rate, m}^3/\text{s},$$

and $\Delta X = \text{measured change in a given quantity.}$

Once the \dot{G}_x are known and the mass-loss rate of the fuel (\dot{M}_f) is calculated using the load-cell assembly, the fractional yield of each combustion product (Y_x) can be calculated by the expression

$$Y_x = \dot{G}_x / \dot{M}_f \quad (2)$$

The Y_x for M_o and N_o of smoke are calculated in a similar manner by the expression

$$Y_x = \Delta X (C_x) (V_oA_o) / \dot{M}_f \quad (3)$$

where $C_x = \text{appropriate units conversion factor: } 1.00 \times 10^{-3}$ when M_o is in milligram per cubic meter or 1.00×10^6 when N_o is in particle per cubic centimeter; and $\Delta X = \text{smoke concentration above ambient (when } M_o \text{ is measured in milligram per cubic meter and } N_o \text{ is measured in particle per cubic centimeter).}$

In an actual mine fire, it is often difficult, if not impossible, to calculate the actual heat of combustion. For flaming fires, the relative hazards tend to increase with the \dot{Q}_A . An indication of the hazard potential can be calculated from the ratio of generation rate to fire size as in the following equation

$$\beta_x = \dot{G}_x / \dot{Q}_A \quad (4)$$

Using the rate of formation of gas or smoke as a function of the fire size is also beneficial in comparing the combustion hazards of different materials.

When the fire size of a certain combustible and its V_oA_o are known, the resultant gas and smoke levels from that material may be calculated from

$$\Delta X = \frac{1}{M_x} (\beta_x) \left[\frac{\dot{Q}_f}{V_oA_o} \right], \quad (5)$$

where $\beta_x = \text{the value for a specific material.}$

For example, if \dot{Q}_f/V_oA_o for a wood fire is known, this equation could be used to calculate the relative gas or smoke concentrations to be expected for wood by using the appropriate value for β_x when ΔX is gas or smoke from wood.

Alternately, one can calculate the \dot{Q}_f/V_oA_o at specified levels of gas or smoke from

$$\frac{\dot{Q}_f}{V_oA_o} = \frac{\Delta X (M_x)}{\beta_x} \quad (6)$$

This last equation is useful for assessing fire intensity at fire sensor alarm thresholds. For example, if a carbon monoxide (CO) sensor has an alarm level of 15 ppm (ΔX) and the emissions are from coal ($\beta_x = 4.8 \times 10^{-3} \text{ g}/\text{kJ}$), then the \dot{Q}_f/V_oA_o is 3.9 at the fire intensity sufficient to produce 15 ppm of CO.

HEAT-RELEASE RATES

All combustion reactions are exothermic. The energy release rate and amount given off is highly variable and depends upon many factors. It has been shown (6) that the \dot{Q}_A rate realized during a fire can be calculated from the expression

$$\dot{Q}_A = \left[\frac{H_C}{K_{CO_2}} \right] \dot{G}_{CO_2} + \left[\frac{H_C - H_{CO} (K_{CO})}{K_{CO}} \right] \dot{G}_{CO}, \quad (7)$$

where $\dot{Q}_A = \text{actual heat release, kW,}$

$H_C = \text{net heat of complete combustion, kJ/g,}$

$H_{CO} = \text{heat of combustion of CO, 10.1 kJ/g,}$

$K_{CO_2} = \text{theoretical yield of } CO_2, \text{ g/g,}$

and $K_{CO} = \text{theoretical yield of CO, g/g.}$

Because each material is unique and has a different carbon content and British thermal unit per pound rating, the theoretical yields of CO and carbon dioxide (CO₂) will vary. The actual values listed in table 2 were derived from an independent testing laboratory. The \dot{Q}_A for each combustible can be calculated by substituting the experimental data for V_oA_o , ΔCO_2 , and ΔCO , and the values from table 2 in equations 1 and 7, which yields:

for wood and jute:

$$\dot{Q}_A = V_oA_o [(0.0216)(\Delta CO_2) + 8.9 \times 10^{-3} (\Delta CO)], \quad (8)$$

transformer fluid:

$$\dot{Q}_A = V_oA_o [(0.0251)(\Delta CO_2) + 7.1 \times 10^{-3} (\Delta CO)], \quad (9)$$

coal:

$$\dot{Q}_A = V_oA_o [(0.0214)(\Delta CO_2) + 8.5 \times 10^{-3} (\Delta CO)], \quad (10)$$

SBR belts:

$$\dot{Q}_A = V_oA_o [(0.0245)(\Delta CO_2) + 1.18 \times 10^{-2} (\Delta CO)], \quad (11)$$

NP belts:

$$\dot{Q}_A = V_oA_o [(0.0238)(\Delta CO_2) + 1.67 \times 10^{-2} (\Delta CO)], \quad (12)$$

PVC belts:

$$\dot{Q}_A = V_oA_o [(0.0258)(\Delta CO_2) + 1.83 \times 10^{-2} (\Delta CO)], \quad (13)$$

PVC brattice:

$$\dot{Q}_A = V_oA_o [(0.0268)(\Delta CO_2) + 1.41 \times 10^{-2} (\Delta CO)], \quad (14)$$

and ducting:

$$\dot{Q}_A = V_oA_o [(0.0216)(\Delta CO_2) + 8.8 \times 10^{-3} (\Delta CO)]. \quad (15)$$

Table 2.—Heat-release equation variables

Material	H _C , kJ/g	K _{CO} , g/g	K _{CO₂} , g/g
Wood	16.4	1.10	1.72
Transformer fluid	40.7	2.03	3.19
Coal	31.0	1.82	2.86
SBR belts	31.0	1.59	2.49
NP belts	23.4	1.23	1.94
PVC belts	24.8	1.21	1.89
PVC brattice	23.5	1.11	1.74
Jute brattice	13.6	.79	1.24
Ventilation ducting	9.0	.52	.82

A typical fire rarely realizes the state of complete combustion. For this reason, the actual heat of combustion (H_A) during a fire is usually less than the total heat of combustion (H_C). By measuring both the \dot{Q}_A , equations 8-15, and the \dot{M}_f , the H_A can be calculated from the expression

$$H_A = \dot{Q}_A / \dot{M}_f. \quad (16)$$

SMOKE INTENSITY PARAMETERS

Smoke evolution is most often expressed in terms of OD, in reciprocal meters. This characteristic provides a measure of fire hazard, in that escape and rescue depend on visibility. It is related to T by the following expression

$$OD = \frac{-1}{\ell} (\ln T), \quad (17)$$

where ℓ = path length in m.

Most smoke detectors are triggered at an OD of 0.1 m⁻¹. The probability of escape and rescue is reduced significantly once the critical level of smoke (OD = 0.5 m⁻¹) has accumulated (7).³

Another measure of smoke hazard is the smoke particle optical density as specific extinction coefficient, ξ . It considers the influence that V_oA_o and \dot{M}_f have on OD. The relationship between ξ and OD is expressed as

$$\xi = \frac{OD}{\dot{M}_f} (V_oA_o). \quad (18)$$

A convenient measurement of smoke density is to examine the obscuration effect of smoke. Some factors influencing obscuration are the number and size of the particles, refractive index, light scattering, ventilation, and distance through which the light must travel. The smoke obscuration is the percentage of light absorbed by the smoke or 100 pct of the light minus the percent T. It is calculated using the following equation:

$$\text{Obscuration} = 100(1 - T). \quad (19)$$

The obscuration values presented in this report are an average of the attenuation of the beam of light at the two wavelengths in the visible range, 0.45 and 0.63 μm .

³Reference 7 quotes a value of OD = 0.218 m⁻¹ for the critical value determined from the expression OD = -1/ℓ log T. When the natural logarithm is used, as in equation 17, then OD = 2.303 × 0.218 = 0.5 m⁻¹, the value used in the text.

SMOKE PARTICLE DIAMETERS

Measurements of both M_o and N_o of the smoke can be used to calculate the average size of the smoke particles, using the expression

$$\frac{\pi d_m^3}{6} (\rho_p)(N_o) = 1 \times 10^3 M_o, \quad (20)$$

where d_m = diameter of a particle of average mass, μm ,

ρ_p = individual particle density, g/cm^3 ,

M_o = particle mass concentration, mg/m^3 ,

and N_o = particle number concentration, p/cm^3 .

Assuming a value of $\rho_p = 1.4 \text{ g}/\text{cm}^3$, then the d_m can be calculated in micrometers from

$$d_m = 11.09 \left(\frac{M_o}{N_o} \right)^{1/3}. \quad (21)$$

Using the three-wavelength smoke detector developed by the Bureau (8), the transmission of the light (T) through the smoke can be calculated for each wavelength. The extinction-coefficient ratio can be calculated for each pair of wavelengths (λ) from the following log-transmission ratios:

$$\frac{\ln T_{\lambda=1.00}}{\ln T_{\lambda=0.63}}, \quad \frac{\ln T_{\lambda=1.00}}{\ln T_{\lambda=0.45}}, \quad \text{or} \quad \frac{\ln T_{\lambda=0.63}}{\ln T_{\lambda=0.45}}$$

Using these extinction coefficients and the curve in reference 8, figure 11, the volume-to-surface mean particle diameter (d_{32}) can be determined. (Calculation of the extinction-coefficient curves assumes spherical particles with an estimated refractive index.) The T must be less than 85 pct before reliable particle sizes can be calculated using this technique.

COMBUSTION HAZARDS

The principal hazards encountered in smoldering combustion involve toxic gas and smoke production. Flaming combustion introduces additional dangers of heat release and flame spread. Tables 3 and 4 give a summary of the fire characteristics for both flaming and smoldering combustion. The gas concentrations and smoke levels have all been obtained during the steady state, when fairly constant values were noted.

Flaming combustion was observed during the wood, coal, transformer fluid, SBR belt, and NP belt experiments. The materials that tended to smolder were jute, PVC brattice, and PVC belts. Four of the eight ventilation ducts resulted in flaming combustion. Their results are listed as ignitable ducting. Two ducts just smoldered. Their results are listed as nonignitable ducting. The thermal decomposition of the remaining two of the ducts sometimes resulted in flaming combustion. Their results are listed in the appropriate combustion designation. Included in the smoldering data are preflaming coal and smoldering plywood and conveyor belts. These smoldering results were obtained from another series of experiments

in which strip heaters were used to keep plywood and conveyor belting in a nonflaming stage.

Table 3.—Gas concentrations, gas ratios, heat-release rates, and heats of combustion

Material	CO, ppm	CO ₂ , ppm	Ratio, CO ₂ /CO	Q _A , kW	H _A kJ/g
FLAMING					
Wood	145	6,759	46.6	110.2	10.6
Transformer fluid ..	113	1,769	15.7	21.1	24.3
Coal	89	1,095	12.3	5.9	15.1
SBR belts	902	13,771	15.3	38.4	16.2
NP belts	112	826	7.4	2.3	2.6
Ignitable ducting ..	700	13,239	18.9	42.5	96.6
SMOLDERING					
Wood	43	ND	ND	ND	ND
Coal	15	19	1.3	0.1	ND
Jute brattice	32	149	4.6	.6	ND
PVC brattice	25	22	.9	.1	ND
Nonignitable ducting	28	139	5.0	.5	ND

ND Not determined.

Table 4.—Smoke characteristics

Material	N_o , 10^6 p/cm ³	M_o , mg/m ³	d_m , μ m	d_{32} , μ m	Obscur- ation, pct	OD, m ⁻¹	ξ , m ² /g
FLAMING							
Wood	6.0	49.1	0.22	ND	9	1.39	0.13
Transformer fluid	1.1	35.3	.39	0.39	46	7.31	3.95
Coal	1.5	11.4	.21	.23	20	2.77	1.70
SBR belts2	43.7	.62	.33	75	15.93	.74
NP belts2	4.7	.30	.30	15	1.63	.20
Ignitable ducting	1.8	224.3	.56	.48	51	7.52	2.56
SMOLDERING							
Wood	ND	50.8	ND	ND	12	1.36	ND
Coal	1.0	3.2	0.16	ND	9	.91	ND
Jute brattice	0.4	6.9	.29	ND	3	.30	ND
PVC brattice	3.0	72.3	.32	0.47	11	1.23	ND
Nonignitable ducts	1.3	32.2	.28	.36	11	1.20	ND

ND Not determined.

The most important narcotic fire gas is CO (9). It is highly toxic because of its affinity to combine with hemoglobin which blocks the uptake of oxygen. Conditions in most fires are normally such that complete oxidation to CO₂ does not occur, thus, some amount of CO is formed. In these experiments, SBR belts and ignitable ducting generated the highest concentrations of CO.

CO₂ is not considered a toxic agent. However, inhalation of CO₂ will stimulate respiration which in turn will lead to increased inhalation of the toxic POC. SBR belts and ignitable ducting lead in the production of CO₂ also. A better indication of combustion efficiency is the CO₂-CO ratio. Most flaming combustion generates predominantly CO₂ with a relatively small amount of CO resulting in a high CO₂-CO ratio. Lower ratios may indicate less efficient combustion such as that resulting from smoldering fires. The flaming combustion of wood produced the highest CO₂-CO ratio.

Other toxic gas products measured in these experiments were hydrogen cyanide (HCN) and hydrogen chloride (HCl). HCN is the most dangerous of the toxic POC after CO because it can interfere with the body's use of oxygen. It is liberated only during the burning of nitrogen-containing materials such as coal. The steady-state production of HCN during these coal experiments averaged 6.5 ± 1.5 ppm. HCL irritates the eyes and upper respiratory tract. It is liberated during the thermal degradation of chlorine-containing materials such as PVC. The average peak production of HCl during the rapid degradation of the PVC brattices was 38 ppm at an average temperature of 283° C. This occurred 3 min after the peak CO production. However, measurable levels of

smoke were recorded 3 min prior to measurable concentrations of either HCl or CO. During the smoldering stage, the steady-state HCl-CO ratio was approximately 4 to 1.

Another hazard occurring in flaming combustion is rapid heat transfer to unburned materials, which promotes flame spread. Its effects can be demonstrated by the combustion of different configurations of wood cribs. The arrangement of the sticks influenced heat transfer. Lowering the crib profile decreased the efficiency of the heat transfer, which produced longer burning times and reduced the mass loss. Lowering the ventilation rate also reduced the heat transfer and mass loss. With less oxygen available, the wood was consumed at a slower rate. In underground fires, it may be beneficial to decrease or stop the airflow, whenever possible. This would slow the progress of the fire by reducing the available oxygen and by lowering the heat released and slow its transfer. An increase in the ventilation once a fire has developed serves only to reoxidize the flames.

Heat of combustion may be defined as the heat produced by the combustion of a given weight or volume of material. This characteristic provides a measure of fire hazard in that a material which burns with the evolution of little heat per unit quantity burned will contribute appreciably less to a conflagration than a material which generates large amounts of heat per unit quantity burned (10). As an example, a fire involving a small amount of ignitable ducting may result in a high actual heat of combustion. Steady-state data in terms of \dot{Q}_A and H_A are listed in table 3. Since wood burned with the greatest \dot{Q}_A , of all the materials tested, as measured by the heat release, the

flaming POC of the other materials were scaled to this fire intensity. These values may be found in table 5. Ignitable ducting produced the highest values, except for N_o which was produced by coal. If ignitable ducting burned at that fire intensity, the most toxic emissions would theoretically result.

Table 5.—Relative¹ gas and smoke values from flaming combustion

Material	CO, ppm	CO ₂ , ppm	N _o , 10 ⁶ p/cm ³	M _o , mg/m ³
Wood	145	6,759	6.04	49.1
Transformer fluid.	284	4,992	2.79	85.2
Coal	441	5,762	7.12	50.6
SBR belts	294	5,017	.01	13.5
NP belts	602	5,009	1.00	22.3
Ignitable ducting.	956	12,393	1.89	294.9

¹Scaled to the fire intensity of wood.

Smoke density provides a measure of fire hazard as well as detectability. The chances of escape and rescue are inversely proportional to the OD. However, the OD of smoke can also be used to alert personnel of potential danger. The thick smoke emitted from burning SBR belts can be compared with the clean burning wood cribs with the resulting escape and detection ramifications. NP belts may be the least hazardous of the flaming combustibles not only because of the low gas and smoke concentrations but also because of the tendency of these belts to self-extinguish.

The average size of the particles is a major factor in smoke obscuration. Two methods of calculating particle size are possible from these determinations. The d_m and d_{32} usually show good agreement. Ignitable ducting and smoldering PVC brattice produced smoke particles with the largest diameter. Wood and coal combustion produced the smallest particles. The smoke characteristics varied slightly between the brands of transformer fluid. One brand produced 52 pct fewer particles than the other

brands. Another brand produced particles with an 82 pct lower M_o . Because of these differences, the d_m ranged from 0.21 to 0.5 μm . The d_{32} had a narrower range from 0.35 to 0.44 μm . However, the average of both diameter determinations was the same, 0.39 μm . The obscuration ranged from 40 to 60 pct. The brand with the largest particle diameters had the highest OD and obscuration.

The POC can also be scaled according to fire size (β_x) or the yield per mass-loss rate (Y_x). Only those materials with significant mass-loss rates and fire sizes were calculated. The β_x values can be found in table 6, and the Y_x values can be found in table 7. These are convenient determinations for assessing the hazardous nature of the emissions. As might be expected, ignitable ducting produced the most toxic emissions per gram of material consumed with wood producing the least. Coal and ignitable ducting produced the most hazardous emissions per kilowatt of heat released.

Table 6.—Production constants from flaming combustion

Material	β_{CO} , 10 ⁻³ g/kJ	β_{CO_2} , 10 ⁻² g/kJ	β_{N_o} , 10 ¹⁰ p/kJ	β_{M_o} , 10 ⁻⁴ g/kJ
Wood	1.6	10.4	5.79	4.9
Transformer fluid.	3.1	7.7	2.48	7.8
Coal	4.8	8.9	6.83	4.7
SBR belts	3.2	7.8	.05	1.2
NP belts	6.6	7.7	.96	2.2
Ignitable ducting.	4.3	8.9	.69	10.7

Table 7.—Production yields from flaming combustion

Material	Y_{CO} , 10 ⁻² g/g	Y_{CO_2} , 10 ⁻¹ g/g	Y_{N_o} , 10 ¹¹ p/g	Y_{M_o} , 10 ⁻³ g/g
Wood	1.7	1.3	5.78	4.7
Transformer fluid.	7.6	1.9	5.94	19.1
Coal	6.8	1.3	9.23	7.0
SBR belts	14.4	3.5	.26	5.6
NP belts	1.8	2.1	.26	.6
Ignitable ducting.	29.8	8.9	6.14	76.5

FIRE DETECTION

Reliable fire detection is an essential aspect of fire protection, both for safe evacuation and fire control or extinguishment. Detection is based on the environmental changes occurring during the combustion process such as the production of heat, light, gases, and smoke. Thermal sensors may be fixed-temperature or rate-of-rise sensors. Optical sensors measure ultraviolet, infrared, or visible

light. POC sensors use chemical changes based on ionization, photoelectric sensing, or gas detection (11). These various types of sensors can be used separately or in combination for a more effective system. The appropriate choice depends on the environmental changes most easily detected. For flaming fires, the speed of detection is another consideration. Transformer fluid fires propagate

immediately, but the dense smoke can be quickly detected. By comparison, the flaming combustion of the wood cribs yielded a clean burning fire with low obscuration rate and OD. Therefore, an optical smoke sensor would not be as effective for detecting fires in areas heavily loaded with wood. However, wood crib fires burn with great intensity which might be expected from the high combustion ratio. Therefore, in areas with large amounts of wood, thermal sensors might be the appropriate choice. In a smoldering wood fire where little heat is generated, smoke sensors would reach their alarm threshold before CO sensors.

The unique fire characteristics of each material present distinct detection dilemmas. The following are examples of different fire scenarios. Coal fires may be preceded by prolonged periods of smoldering such as when spontaneous combustion or self-heating occurs. Fire detection under these circumstances may not be as critical, but must still be reliable. This type of fire, if left undetected, can become a dangerous and life-threatening situation. The smoke of coal fires seems to be most easily detected POC.

SBR is a very flammable copolymer with high mechanical strength when reinforced with carbon black. Since conveyor belts are subject to friction ignition, flammability can be reduced by the incorporation of a combination of flame retarding additives which, unfortunately, tend to increase the formation of smoke and toxic products. The high obscuration rate and OD observed are evidence of this smoke-producing characteristic which can be readily detected.

Although rigid PVC is not very flammable because of its high chlorine content, significant amounts of flammable plasticizers can be added to increase flexibility. Consequently, flame retardants are incorporated into the polymer to reduce flammability. Unfortunately, in some cases, the addition of fire retardants results in a decreased tendency to ignite, but an increasing tendency to smoke when ignition finally takes place (12). In the manufacturing process, a compromise formulation must be reached to achieve either reduced smoke formation or low flammability depending upon the intended application. Smoldering PVC brattice produced smoke with rather large particle diameters and relatively high OD. For either PVC belts or brattice, smoke detection would be the appropriate choice.

As demonstrated, the selection of a CO sensor verses smoke detector can be simplified when the relative quantities of the POC are measured. If one assumes

that a typical CO fire sensor has a maximum alarm threshold level of 15 ppm above ambient, and a typical smoke fire sensor has a maximum alarm threshold level of 0.1 m^{-1} OD, then the data in tables 1, 3, and 4 can be used to estimate fire sizes at which these levels of CO and smoke are expelled into the ventilation airflow. Table 8 makes this comparison for flaming combustion as a function of \dot{Q}_f/V_oA_o using equation 19 and the average ratio of smoke OD to ppm CO for the materials tested (column 2 of table 8).

Table 8.—Sensor alarm ratios and fire intensity at sensor alarm for flaming combustion

Material	OD, (m^{-1})/ppm CO	\dot{Q}_f/V_oA_o , $\text{kJ}/\text{m}^3 \text{ at—}$	
		15 ppm CO	0.1 m^{-1} OD
Wood	0.0096	11.7	8.15
Transformer fluid.	.0647	6.0	.62
Coal0311	3.9	.84
SBR belts0255	5.9	1.53
NP belts0146	2.8	1.29
Ignitable ducting.	.0107	4.4	2.71

From table 8, at a constant V_oA_o , CO fire sensors would detect a smaller NP belt fire than any of the other flaming combustibles. Smoke fire sensors would detect a transformer fluid fire with a low fire intensity better than any other flaming combustible. Detectable fire intensities for wood are significantly greater than for the other materials, indicating that this type of fire is more difficult to detect. Smoke sensor alarm thresholds are reached at smaller ratios than CO alarm thresholds.

To assist in determining which type of fire sensor (smoke or CO) is more effective for smoldering materials, a comparison can be found in table 9. A smoke sensor is the obvious choice because the OD of the smoke is well above the alarm threshold of 0.1 m^{-1} by the time the CO threshold of 15 ppm is reached. Jute brattice is the only exception, with smoke detection only slightly ahead of CO detection. However, for all materials tested, the CO concentration had not reached alarm levels by the time the OD had more than surpassed its alarm threshold. Table 10 ranks mine combustibles for ease of fire detection. The combustion emissions detected by a CO sensor are in the reverse order of smoke detection and that all the combustibles tested are more readily detected by smoke (OD) than by CO concentration.

Table 9.—Relative levels of CO and smoke at respective alarm thresholds for smoldering combustion

Material	OD, 15 ppm CO	CO, 0.1 m ⁻¹ OD
PVC belts	1.52	0.99
SBR belts	1.42	1.05
NP belts	1.05	1.44
Coal91	1.65
PVC brattice72	2.10
Nonignitable ducting.64	2.33
Wood47	3.16
Jute brattice14	10.67

Table 10.—Detectability ranking of smoldering mine combustibles

Material	CO sensor	Smoke sensor
Jute brattice	1	8
Wood	2	7
Nonignitable ducting.	3	6
PVC brattice	4	5
Coal	5	4
NP belts	6	3
SBR belts	7	2
PVC belts	8	1

CONCLUSIONS

Burning materials generate unique and dangerous POC. These experiments were conducted to measure the smoke and gas generated and to compare their potential detectability. The following combustion characteristics were derived from this series of experiments. Burning wood cribs liberated the most heat as was expected from the high M_p . Transformer fluid fires can quickly produce critical smoke and propagation levels which make them readily detectable, but limit escape and rescue efforts. SBR belts produced dense smoke evidenced by the high obscuration rate and OD. NP belts may support flame propagation (given the proper conditions) even though considered self-extinguishing. Ignitable ventilation ducting produced the largest M_o resulting in large d_m and on a relative scale produced the highest amounts of CO and CO₂. Burning PVC belt and brattice emissions have

increased toxicity because of the release of HCl. Smoldering jute brattice releases small amounts of CO and smoke and could, therefore, go undetected. Smoke detection proved only slightly more effective than CO detection. Nonignitable ventilation ducting may be one of the safest materials underground because it is difficult to ignite and does not support flame propagation. However, if consumed in a fire, it could add toxic components to the combustion product mixture. In a mine fire, these products combine to produce a wide variety of smoke particles and volatile gases that are transported by the ventilation system. Because of the unique nature of underground mining, fire detection is of utmost importance. For the materials tested, smoke sensors are more effective for fire detection because their alarm thresholds are reached before that of the CO sensors.

REFERENCES

1. Egan, M. R., and C. D. Litton. Wood Crib Fires in a Ventilated Tunnel. BuMines RI 9045, 1986, 18 pp.
2. Egan, M. R. Transformer Fluid Fires in a Ventilated Tunnel. BuMines IC 9117, 1986, 13 pp.
3. _____. Coal Combustion in a Ventilated Tunnel. BuMines IC 9169, 1987, 13 pp.
4. _____. Emission Products From Combustion of Conveyor Belts. BuMines IC 9205, 1988, 12 pp.
5. _____. Thermal Decomposition of Ventilation Ducting. BuMines IC 9263, 1990, 11 pp.
6. Tewarson, A. Generation of Heat and Chemical Compounds in Fires. Ch. in The SFPE Handbook of Fire Protection Engineering, ed. by P. E. DiNenno. Natl. Fire Prot. Assoc., 1st ed., 1988, pp. 1-179 to 1-199.
7. Tewarson, A., and J. S. Newman. An Experimental Investigation of the Fire Hazards Associated With Timber Sets In Mines. Paper in Proceedings: Bureau of Mines Technology Transfer Seminars, Denver, CO, Nov. 3, 1981, and St. Louis, MO, Nov. 6, 1981. BuMines IC 8865, 1981, pp. 86-103.
8. Cashdollar, K. L., C. K. Lee, and J. M. Singer. Three-Wavelength Light Transmission Technique To Measure Smoke Particle Size and Concentration. Appl. Optics, v. 18, No. 11, 1979, pp. 1763-1769.
9. Purser, D. A. How Toxic Smoke Products Affect the Ability of Victims to Escape From Fires. Fire Prev., No. 179, 1985, pp. 28-32.
10. Hilado, C. J. (ed.). Flammability Handbook for Plastics. Technomic Publ., 3d ed., 1982, p. 118.
11. Pomroy, W. H. Fire Detection Systems for Noncoal Underground Mines. Paper in Recent Developments in Metal and Nonmetal Fire Protection. BuMines IC 9206, 1988, p. 21.
12. Landrock, A. H. Handbook of Plastics Flammability and Combustion Toxicology. Noyes Publ., 1983, p. 95.

APPENDIX.—SYMBOLS USED IN THIS REPORT

d_m	diameter of a particle of average mass, μm	p	particle
d_{32}	volume-to-surface mean particle size, μm	\dot{Q}_A	actual heat-release rate, kW
\dot{G}_X	generation rate of a given combustion product, g/s or p/s	\dot{Q}_f	heat-release rate of the fuel, kW
H_A	actual heat of combustion, kJ/g	T	transmission of light, pct
H_C	net heat of combustion of the material, kJ/g	V_oA_o	ventilation rate, m^3/s
H_{CO}	heat of combustion of CO, kJ/g	Y_X	yield of a given combustion product, g/g or p/g
K_X	theoretical yield of a given gas, g/g	β_X	production constant of a given combustion product, g/kJ or p/kJ
ℓ	optical path length, m	Δm	measured change in mass, g
\ln	logarithm, natural	Δt	measured change in time, s
\dot{M}_f	mass loss, g	ΔX	measured change in a given quantity
M_o	particle mass concentration, mg/m^3	λ	wavelength of light source, μm
M_X	conversion unit for generation rates	ξ	specific extinction coefficient or particle optical density, m^2/g
N_o	particle number concentration, p/cm^3	ρ_p	individual particle density, g/cm^3
OD	optical density per unit path length, m^{-1}		